7th International Building Physics Conference

IBPC2018

Proceedings

SYRACUSE, NY, USA

September 23 - 26, 2018

Healthy, Intelligent and Resilient Buildings and Urban Environments

ibpc2018.org | #ibpc2018

Comparison of Lattice Boltzmann Method and Finite Volume Method with Large Eddy Simulation in Isothermal Room Flow

Mengtao Han[1,*], Ryozo Ooka[2] and Hideki Kikumoto[2]

[1] JSPS Research Fellow, School of Engineering, the University of Tokyo, Japan
[2] Institute of Industrial Science, the University of Tokyo, Japan

[*]*Corresponding email: hanmt@iis.u-tokyo.ac.jp*

ABSTRACT
Lattice Boltzmann method (LBM), as a new computational fluid simulation method, has aroused widespread attention in recent decades within engineering practice. LBM with large eddy simulation (LBM-LES) model is commonly used in predicting high Reynolds flow, and is considered to have a prediction accuracy similar to traditional finite volume method (FVM-LES). Nonetheless, a systematic discussion on the accuracy of LBM-LES, and its consistency with FVM-LES, in indoor turbulent flow situations, is still insufficient. In this study, simulations of an indoor isothermal forced convection benchmark case (from IEA Annex 20) are implemented by using both LBM-LES and FVM-LES, with the aim of comparing the accuracies of LBM-LES and FVM-LES, in indoor turbulent flow situations. A comparison of their relative computation speeds, and parallel computation performances, is also implemented. The results show that LBM-LES can achieve the same level of accuracy as FVM-LES, in indoor turbulent flow situations; however, more refined meshes are required. Compared with FVM-LES, half size grids are required for LBM-LES to approach similar levels of accuracy, meaning that the meshes of LBM-LES are approximately eight times as large as FVM-LES. The computation speeds of both LBM-LES and FVM-LES scale well, with the increase in the number of computation cores in one node. Their computation speeds (with the same accuracy) approach a similar level; however, the parallel computation speed of the LBM-LES speed can be larger than FVM, owing to its superior parallel speedup performance.

KEYWORDS
Lattice Boltzmann method, Finite volume method, Large-eddy simulation, Indoor turbulent flow

INTRODUCTION
The lattice Boltzmann method (LBM) has recently been applied in indoor turbulent flows (Sajjadi et al. 2016), in place of the conventional finite volume method (FVM). Based on the lattice Boltzmann equation, the LBM simulates the fluid motion process by assuming a collection of particles colliding, and a stream behavior for their distribution functions (Chen and Doolen 1998). When solving turbulent flow problems with a high Reynolds number, the LBM can be used with a large eddy simulation (LBM-LES) model, as in the FVM (FVM-LES). As it is necessary to solve the Poisson equation in the FVM, there is an obvious disadvantage in that the calculation load and time cost are tremendous. However, the LBM shows more promise in high-speed LES simulations for complex and large-scale urban flows, owing to its simpler algorithm, and it is also more appropriate for parallel calculations.

Although the LBM has been applied in the flow simulation of indoor turbulence, a systematic comparison of its accuracy, consistency, and computation speed with the FVM is still insufficient. Therefore, in this research, simulations of an indoor turbulent flow benchmark case from IEA Annex 20 (Lemaire et al. 1993) are implemented by using both the LBM-LES and

FVM-LES, to verify the accuracy of the LBM-LES and to compare this accuracy with that of FVM-LES. The computation speeds and parallel computation performances are also determined.

OUTLINE OF LBM

Lattice Boltzmann equation

Instead of the Navier-Stokes equation, the LBM in this research simulates the fluid using the lattice Boltzmann equation, with the BGK approximation (Bhatnagar, Gross, and Krook 1954). The non-external-force lattice Boltzmann-BGK equation is expressed as Equation (1), where Δt is the discrete time, $\mathbf{e}_a$ is the discrete speed in the a-direction, $f_a(\mathbf{r},t)$ is particle a s distribution function, $f_a^{eq}(\mathbf{r},t)$ is the equilibrium function, and τ is the relaxation time.

$$f_a(\mathbf{r}+\mathbf{e}_a\Delta t, t+\Delta t) - f_a(\mathbf{r},t) = \frac{1}{\tau}\left[f_a^{eq}(\mathbf{r},t) - f_a(\mathbf{r},t)\right] \quad (1)$$

Discrete velocity scheme

The DdQq (d = spatial dimension, q = discrete particle speed) discrete velocity scheme (Qian, D Humières, and Lallemand 1992) is widely accepted for the LBM. In this research, the D3Q19 scheme was employed, as shown in Figure 1. Cubic lattices are used in this scheme, with 18 adjacent points for every lattice point. The particles only exist on the points, and move to an adjacent point, or just rest, during each time step. Therefore, the D3Q19 scheme has three types of particles, with motion speeds indicated in Table 1, where e is the particle speed, $e = \Delta x/\Delta t$, and Δx is the lattice length.

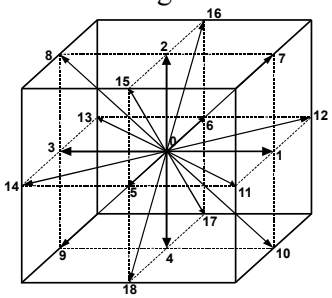

Figure 1. Lattice system of the D3Q19 scheme

Table 1. Discrete velocity of each particle

Particle No.	Discrete velocity	Motion paths
0	0	rest
1– 6	e	along the normal axis
7– 18	$\sqrt{2}\,e$	along the diagonal

LES model in LBM

In this study, the LES (using the standard Smagorinsky SGS model) is implemented. According to the LES theory, the total viscosity ν_{total} is composed of the molecular viscosity ν and the eddy viscosity ν_t. The ν_{total} and ν_t are given by Equation (2).

$$\nu_{total} = \nu + \nu_t, \qquad \nu_t = (C_s\Delta)^2|\bar{s}| \quad (2)$$

where C_s is the Smagorinsky constant, Δ is the filter, and $\bar{s}$ is the strain rate tensor. This is as same as the LES theory of the FVM.

Furthermore, the total viscosity can be calculated using Equation (3) by the LBM s theory.

$$\nu_{total} = {e_s}^2(\tau_{total} - 0.5)\Delta t \quad (3)$$

where e_s is the speed of sound of the particles, and τ_{total} is the total relaxation time. Therefore, the total relaxation time τ_{total} is obtained from ν_{total}, and it substitutes the original relaxation time τ in Equation (1), to implement the LBM-LES simulation.

OUTLINE OF SIMULATION TARGET AND SIMULATION CONDITIONS

The LBM-LES and FVM-LES (abbreviated to LBM and FVM below) approach was conducted for the indoor isothermal forced flow. The room model and simulation boundary conditions are shown in Figure 2 and Table 2, respectively. The room characteristics are $L / H = 3,\ h / H = 0.056,\ t / H = 0.16$, and $Re = 5000$, where L, H, h, t and Re represent the room length, room height, slot inlet height, outlet height, and the Reynolds number (refer to the inlet height and velocity), respectively. Since the inlet turbulence intensity of the experimental data is only 4% according to the IEA report, it can be considered to have a very small impact on the velocity, and thus, the inlet turbulence intensity was ignored in this simulation. A set of various uniform grid resolutions were employed, as illustrated in Table 3.

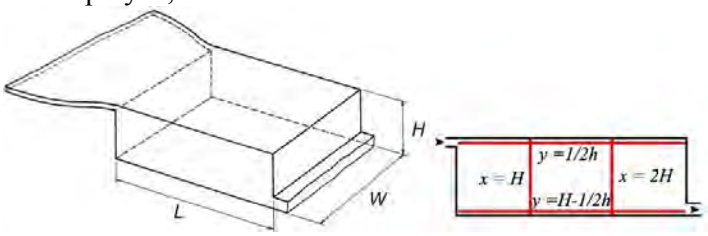

Figure 2. Sketch of the simulation target (from IEA Annex 20)

Table 2. Boundary conditions (B.C.)

Item	FVM-LES	LBM-LES
Sub-grid scale model	Standard Smagorinsky model (C_s= 0.12)	
Damping function	Van Driest-style	
Simulation domain	9.0 m (L) ×3.0 m (W) ×3.0 m (H)	
Time discretization	Euler-implicit	-
Space discretization	2nd-order central difference	-
Simulation Period	Preparatory: 18 min, average: 6 min (air change rate: 0.172 min^{-1})	
Inlet B.C.	Uniform velocity boundary, $\boldsymbol{U}_{in} = 0.455\ m/s$, (no fluctuations)	
Outlet B.C.	Gradient-zero	
Other B.C.	Wall function (Spalding s law)	No-slip (Bounce-back)

Table 3. Case study

Case Name	Simulation Method	Grid size	Mesh quantity
LBM_004	LBM-LES	0.04 m (1/75 *H*)	1.6 M
LBM_002		0.02 m (1/150 *H*)	10.1 M
LBM_001		0.01 m (1/300 *H*)	81 M
FVM_004	FVM-LES	0.04 m (1/75 *H*)	1.6 M
FVM_002		0.02 m (1/150 *H*)	10.1 M

RESULTS AND DISCUSSIONS

Time-averaged scalar velocity

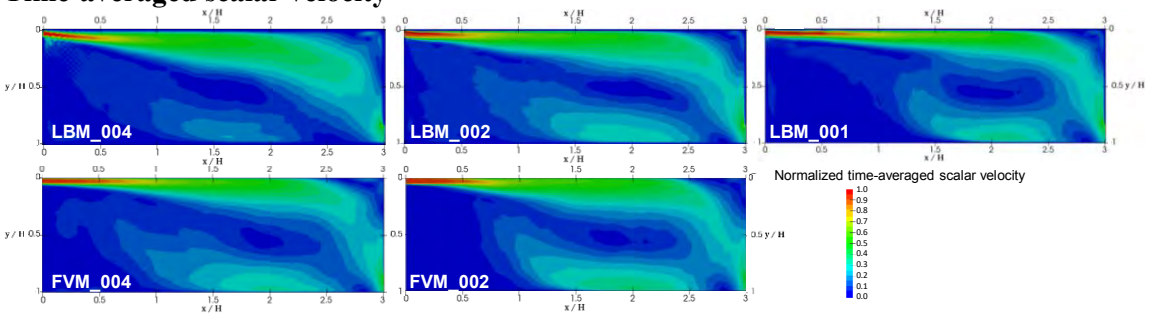

Figure 3. Normalized time-averaged scalar velocity of each cases

Figure 3 shows the normalized time-averaged scalar velocity of the central vertical section for the different cases. A large air circulation flow, which was equivalent to the room size, occurred

from the inlet, with a region-stagnated air flow in the center of the room. The LBM represented the flow features as well as the FVM. Nonetheless, a tendency of moving lower away from the ceiling, for the airflow from the inlet, could be observed clearly in LBM_004. This is most probably because the LBM employed the standard bounce-back boundary condition, which excludes a wall function (such as the Spalding rule) for calculating the eddy viscous drag at the wall layer. Also, the damping function (such as the Van Driest style) is absent from the LBM, causing an overestimation of the eddy viscosity adjacent to the ceiling compared with the FVM, and it weakened as the LBM s grids became finer. This phenomenon did not occur in the FVM, regardless of grid resolutions, since the wall function and the damping function was employed.

Comparison of the accuracy of LBM and FVM

The experimental data (Nielsen, Rong, and Olmedo 2010) was used to validate the accuracy. As shown in Figure 4, both LBM and FVM were generally able to represent the distribution tendency of $\langle U \rangle$ (the mainstream direction component of the time-averaged mean velocity), except for LBM_004, which demonstrated the most unacceptable accuracy. The LBM s accuracy improved as the grid resolutions improved in each region. For $x = H$, the velocities of all the LBM cases were under-predicted in the jet, most probably due to the absence of the damping function, while the FVM agreed well. Further, both LBM and FVM slightly underestimated the velocity on the height of the inlet at $x = 2H$, and the same was true along $y = 1/2h$. Along $y = H - 1/2h$, LBM cases agreed well with the experiment, as did the FVM.

Figure 4 shows the comparison of the RMS profiles of the horizontal velocity component ($\text{RMS} = \sqrt{\langle u'^2 \rangle}$). Near the ceiling, at $x = H$, FVM overestimated the RMS, while the accuracy of the LBM was higher (especially LBM_001). Along $y = 1/2h$, the FVM also over-predicted the RMS, and the LBM achieved a higher accuracy. On the other hand, both the LBM and FVM underestimated the RMS at the lower area, at $x = 2H$ and along $y = H - 1/2h$. This underestimation of the RMS also appeared in the FVM-LES implemented by Davidson (Davidson and Nielsen 1996). In addition, because both the LBM and FVM demonstrated an underestimation at these areas, it may not be not an inherent problem of the LBM, but rather due to a difference between the simulations and experimental conditions.

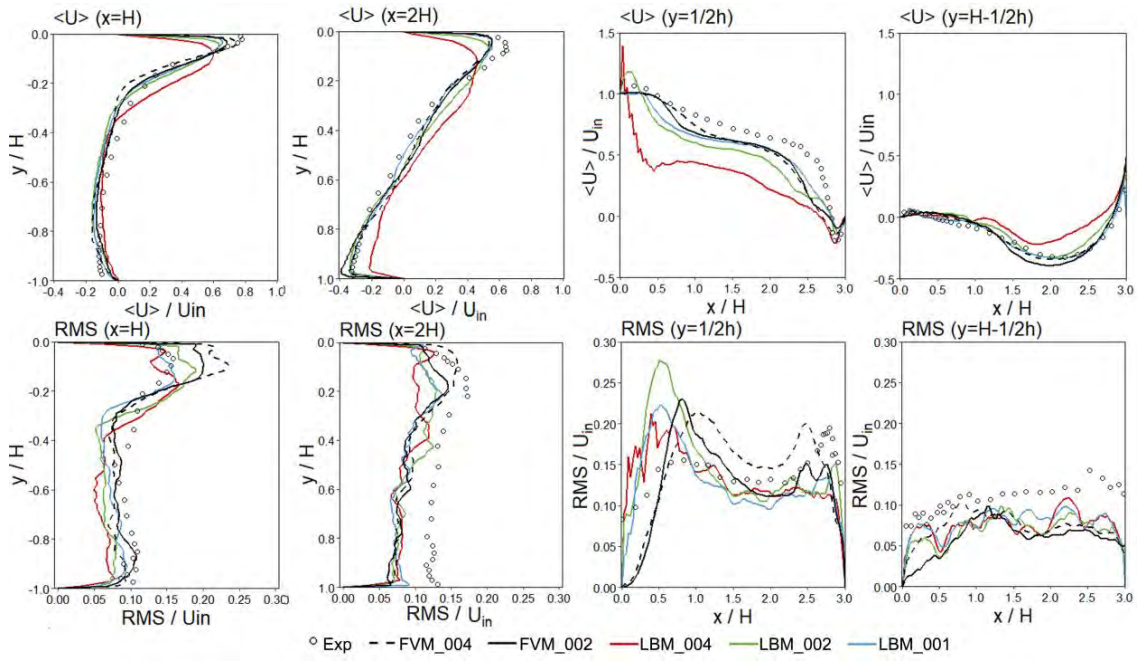

Figure 4. Distribution of $\langle U \rangle$ (top row) and RMS (bottom row)

The accuracy of simulations is quantitatively evaluated by considering all the experimental and predicted data of the corresponding spots, using the mean error (ME) defined by Equation (4), where $V_{EXP(i)}$ and $V_{LBM\ or\ FVM\ (i)}$ are the experimental or predicted data of corresponding spots.

$$\mathrm{ME} = \frac{1}{M}\sum_{i=1}^{M}\left|V_{LBM\ or\ FVM(i)} - V_{EXP(i)}\right| \tag{4}$$

Figure 5 shows the ME of the measurement points at all the points (All Data), the points adjacent to the ceiling ($y = 1/2h$), the ground ($y = H - 1/2h$), and points far away from walls ($x = H, 2H$). Generally, among all the LBM cases, the accuracy of $\langle U \rangle$ was markedly improved when the grid resolution was changed from 0.04 m to 0.02 m, but only slightly improved when it was changed from 0.02 m to 0.01 m. The accuracy of the FVM cases was between that of LBM_002 and LBM_001. With respect to RMS, the accuracy of the LBM was almost the same at any grid resolution and was slightly better than the FVM. Whether for all points, or sub-regional points, the previous tendency was clearly observed. With regard to the sub-regional points MEs (for $\langle U \rangle$), the maximum and minimum MEs appeared adjacent to the ceiling ($y = 1/2h$) and to the ground ($y = H - 1/2h$), respectively, regardless of simulation methods and grid resolutions. The difference in RMS among different sub-regions was small.

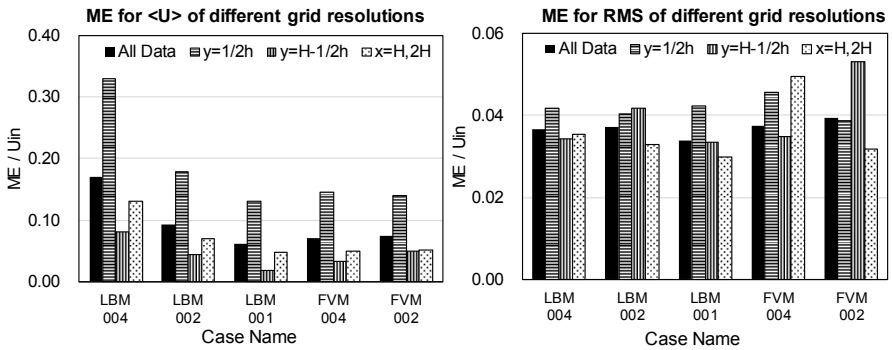

Figure 5. Mean Error (ME) of different grid resolutions

In conclusion, the same grid resolution of the LBM and FVM led to different accuracy levels in this study. More refined grids were required for the LBM to achieve the same accuracy than the FVM. The accuracy of LBM_002 and LBM_001 approximated that of FVM_004 and FVM_002, respectively, showing that the LBM required half the grid width of the FVM.

COMPUTATION SPEED AND PARALLEL COMPUTATION PERFORMANCE

The computation speeds, and parallel computation performances attained using the two methods, were compared using one node including two Intel (R) Xeon (R) E5-2667v4 @ 3.20 GHz (8 cores) CPUs, and the simulations were performed with different core utilization situations (1, 2, 4, 8, and 16). The elapsed computation time was normalized by the physical time for the flow motion (24 min), as shown in Figure 6. The computation times of both the LBM and FVM linearly decreased (approximately) with the increase in the cores, indicating that their speeds scaled well. The computation times of LBM_002 and LBM_001 were of almost the same order as those of FVM_004 and FVM_002, respectively, signifying that for the same accuracy, LBM and FVM used the same amount of computation time.

Figure 7 shows the LBM s computation speed ratio of the FVM of LBM and FVM with different core usage situations, and parallel efficiency for both the FVM and LBM. The computation speed of the LBM using one core was only 0.4 times that of the FVM, but it increased with increase in the number of cores, and finally became about 1.2 when the number

of cores approached 16. Although the parallel efficiency of both the LBM and FVM had initial values of 2-3, the parallel efficiency of the LBM increased to 24, whereas that of the increased only to 9. This signified that the parallel efficiency of the LBM responded much better to an increase in the number of cores.

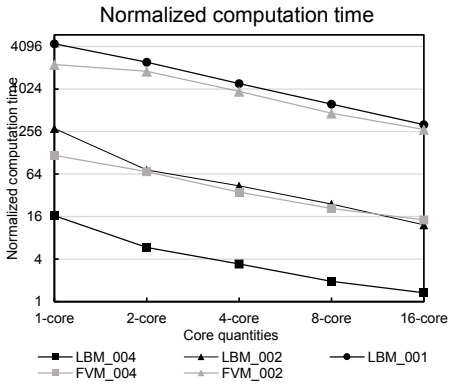

Figure 6. Normalized computation time

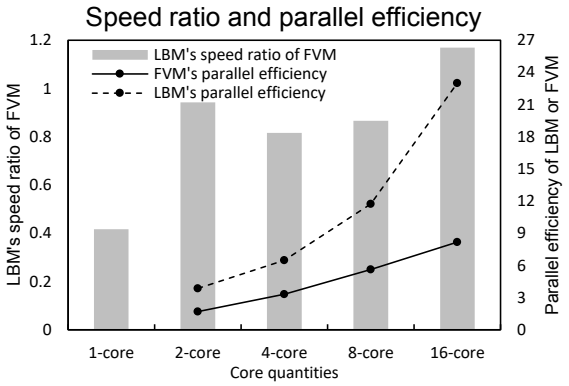

Figure 7. Parallel computation efficiency

CONCLUSIONS

In the indoor turbulent flow situation, the LBM can accurately represent the physical flow structure, and this accuracy improves as the grid resolution becomes higher. The grid width needed for the LBM is approximately half that of the FVM, to achieve the same level of accuracy, partly due to the absence of the wall function in the LBM. Regarding the computation speeds, the speeds of both the LBM and FVM scaled well with an increase in cores quantity in one node. The speeds of LBM and FVM were on approximately the same level for the same degree of accuracy, even though the LBM s mesh was 8 times that of the FVM s. The speed of the LBM corresponding to 1-core is much slower than the FVM, while the speeds corresponding to 16-core became faster due to the better parallel simulation performance of the LBM. Furthermore, the LBM parallel speedup scales well with the increase in the cores, whereas FVM suffers from an upper limitation. Therefore, the speed of the LBM may be further increased by employing more cores (for e.g., in supercomputers); this will be considered in future research.

ACKNOWLEDGEMENT

This research was partially supported by the Research Fellowships program of the JSPS for Young Scientists (KAKENHI Grant Number 18J13607, general manager: Mengtao Han).

REFERENCES

Bhatnagar, P. L., E. P. Gross, and M. Krook. 1954. “A Model for Collision Processes in Gases. I. Small Amplitude Processes in Charged and Neutral One-Component Systems.” *Physical Review* 94 (3): 511–25.

Chen, Shiyi, and Gary D Doolen. 1998. “Lattice Boltzmann Method for Fluid Flows.” *Annual Rev. Fluid Mechanics* 30 (Kadanoff 1986): 329–64. doi:10.1146/annurev.fluid.30.1.329.

Davidson, Lars, and Peter V Nielsen. 1996. “Large Eddy Simulations of the Flow in a Three-Dimensional Ventilated Room.” *5th Int. Conf. on Air Distributions in Rooms ROOMVENT ’96* 2: 161–68.

Lemaire, A.D., Qingyan Chen, M. Ewert, Jorma Heikkinen, C. Inard, Alfred Moser, Peter Vilhelm Nielsen, and G. Whittle. 1993. “Room Air and Contaminant Flow, Evaluation of Computational Methods, Subtask-1 Summary Report.” *IEA Annex 20: Air Flow Patterns within Buildings*, 82.

Nielsen, Peter V, Li Rong, and Inés Olmedo. 2010. “The IEA Annex 20 Two-Dimensional Benchmark Test for CFD Predictions.” *Clima 2010, 10th REHVA World Congress*, 978-975-6907-14–16.

Qian, Y. H., D. D Humières, and P. Lallemand. 1992. “Lattice Bgk Models for Navier-Stokes Equation.” *Epl* 17 (6): 479–84.

Sajjadi, H, M Salmanzadeh, G Ahmadi, and S Jafari. 2016. “Simulations of Indoor Airflow and Particle Dispersion and Deposition by the Lattice Boltzmann Method Using LES and RANS Approaches.” *Building and Environment* 102. Elsevier Ltd: 1–12.